

Dalton Transactions

Accepted Manuscript



This is an *Accepted Manuscript*, which has been through the Royal Society of Chemistry peer review process and has been accepted for publication.

Accepted Manuscripts are published online shortly after acceptance, before technical editing, formatting and proof reading. Using this free service, authors can make their results available to the community, in citable form, before we publish the edited article. We will replace this *Accepted Manuscript* with the edited and formatted *Advance Article* as soon as it is available.

You can find more information about *Accepted Manuscripts* in the [Information for Authors](#).

Please note that technical editing may introduce minor changes to the text and/or graphics, which may alter content. The journal's standard [Terms & Conditions](#) and the [Ethical guidelines](#) still apply. In no event shall the Royal Society of Chemistry be held responsible for any errors or omissions in this *Accepted Manuscript* or any consequences arising from the use of any information it contains.

Structural and Magnetic Studies of Perovskite $\text{YCr}_{0.5}\text{Mn}_{0.5}\text{O}_3$.**Hannah James, Brendan J. Kennedy* and Thomas A. Whittle***School of Chemistry, The University of Sydney, Sydney, NSW 2006, Australia***Maxim Avdeev***Australian Nuclear Science and Technology Organisation, Lucas Heights, NSW 2234, Australia***Abstract**

The structure of $\text{YCr}_{0.5}\text{Mn}_{0.5}\text{O}_6$, established from Rietveld refinement of powder neutron diffraction data, contains Cr and Mn that are disordered on the octahedral sites. The structure is best described in the orthorhombic space group $Pbnm$. Low temperature neutron diffraction data reveal a G-type antiferromagnetic type arrangement, with a ferromagnetic component along the b -axis, indicating that the Cr and Mn couple ferro (or possibly ferri) magnetically to each other.

Introduction

The complex interplay between the spin, orbit, lattice and charge degrees of freedom in doped manganese perovskites results in examples of unique and fascinating phenomena, including colossal magnetoresistance, magnetocaloric response and multiferroic behaviour.¹ Orbital ordering in Mn^{3+} perovskites is a consequence of a Jahn-Teller type distortion², that is also evident in Cu^{2+} ($3d^9$) perovskites, where it is related to the observed superconducting behaviour.

The title oxide Y_2CrMnO_6 has recently become of interest, however the structure of this is not well established. Liu and co-workers³ described it as having an orthorhombic structure in space group $Pnma$ (an alternate setting of $Pbnm$) where the Cr^{3+} and Mn^{3+} cations are disordered on the octahedral sites. If the two cations are disordered it is best to describe this as $\text{YCr}_{0.5}\text{Mn}_{0.5}\text{O}_3$ to emphasise the disorder. Independently Hao and co-workers^{4,5} argued that the Cr^{3+} and Mn^{3+} cations were ordered, suggesting two monoclinic structures initially in $P2_1/n$ but later revising this to $P2_1/b$. The cation ordered arrangement is best represented by the formula Y_2CrMnO_6 . These two monoclinic structures differ in the arrangement of the Cr^{3+} and Mn^{3+} cations, the former having a rock-salt like ordering whereas the latter has a layered ordered arrangement. Both Liu³ and Hao^{4,5} relied on X-ray diffraction to establish the structure of $\text{YCr}_{0.5}\text{Mn}_{0.5}\text{O}_3$. The applicability of this approach is questionable since the electron configuration of Cr^{3+} and Mn^{3+} differ by a single electron; consequently Cr^{3+} and Mn^{3+} are practically indistinguishable when investigated using conventional X-ray diffraction methods.

Ordering of cations in perovskites typically requires a significant difference in the ionic size and/or charge of the cations⁶ as illustrated in Sr_2NiWO_6 ⁷ Charge ordering occurs in oxides such as $\text{Ba}_2\text{Bi}^{\text{III}}\text{Bi}^{\text{V}}\text{O}_6$.⁸ Orbital ordering can also occur leading to a lowering of symmetry as illustrated in the vanadates AVO_3 .⁹ Cation ordering, irrespective of its origin, is often associated

with unusual electronic properties¹⁰ and the ferrimagnetism reported for $\text{YCr}_{0.5}\text{Mn}_{0.5}\text{O}_3$ may provide evidence of this. Whilst there are numerous examples of cation ordering in perovskite-type oxides⁶, ordering of Cr^{3+} and Mn^{3+} in a perovskite would be exceptional, given the similarity in the size and charge of these two cations and would be a unique example of orbital effects inducing chemical ordering. Given the absence of any well known examples of such ordering there is a need to establish if such ordering does indeed occur.

In the present paper we have utilised powder neutron diffraction to establish a precise and accurate structure of $\text{YCr}_{0.5}\text{Mn}_{0.5}\text{O}_3$. Whilst the X-ray scattering factors of Cr^{3+} and Mn^{3+} are extremely similar the neutron scattering lengths are dramatically different Mn has a coherent scattering factor of -3.73 fm and Cr has a coherent scattering factor of 3.635 fm. The magnetic structure of $\text{YCr}_{0.5}\text{Mn}_{0.5}\text{O}_3$ has also been investigated.

Experimental

A 5 g sample of $\text{YCr}_{0.5}\text{Mn}_{0.5}\text{O}_3$ was prepared by the solid state synthesis of Y_2O_3 , Cr_2O_3 and Mn_2O_3 . After drying the oxides, stoichiometric quantities of Y_2O_3 , Cr_2O_3 and Mn_2O_3 were mixed in an agate mortar and pestle under acetone. The resulting mixture was transferred to an alumina boat and then heated overnight in air at 1173 K, and then, after regrinding, at 1473 K for 24 hours using a muffle furnace. The powder was reground, pressed into pellets at heated at 1673 K for 96 hours with periodically re-grounding and pelleting until the powder X-ray diffraction pattern no longer changed. The sample cooled to room temperature in the furnace over a period of ~ 5 hours. The final product was black.

Magnetic measurements were conducted between 4 K and 300 K under both field cooled and zero field cooled conditions with a measuring magnetic field of 1 kOe using a Quantum Design Physical Properties Measurement System. Magnetic hysteresis loops were measured at 5 K.

X-ray diffraction data were collected on a PANalytical X'Pert Pro MPD X-ray diffractometer (45 kV, 40 mA). Data were collected for a 2θ range of 5 to 120° using $\text{CuK}\alpha$ radiation. Neutron powder diffraction data were measured using the high resolution powder diffractometer Echidna at ANSTO's OPAL facility at Lucas Heights using wavelengths of 1.622 or 2.439 Å.¹¹

Results and Discussion

A polycrystalline sample of $\text{YCr}_{0.5}\text{Mn}_{0.5}\text{O}_3$ was prepared as described by Hao *et al.*⁴. The extent of cation disorder in perovskites can be influenced by the highest temperature used to prepare the sample and the rate of cooling, with rapid cooling tending to stabilise disordered structures. The present sample was heated to 1673 K, the same maximum temperature employed by Hao *et al.*⁴, and the sample was slowly cooled. The structure of this was initially investigated using powder X-ray diffraction (XRD) data. As described by Liu *et al.*³ and Hao *et al.*⁴ Rietveld refinement assuming a disordered arrangement of the Cr and Mn cations in the orthorhombic *Pbnm* space group was successful. Examination of the data revealed a weak peak near $2\theta = 30^\circ$ that was identified as coming from the presence of a small amount of Y_2O_3 , Liu *et*

al. noted that high pressure was required to eliminate the formation of this phase.³ Models in the two monoclinic models described by Hao *et al.* ($P2_1/n$ and $P2_1/b$)^{4,5} were also tested and these gave comparable quality fits to the XRD data, reflecting the similarity in the X-ray scattering factors of Cr^{3+} and Mn^{3+} . The same cannot be said for the neutron powder diffraction (NPD) data. Figure 1 illustrates a portion of the powder neutron diffraction pattern for $\text{YCr}_{0.5}\text{Mn}_{0.5}\text{O}_3$ recorded at room temperature.

The models for the $P2_1/b$ and $P2_1/n$ symmetries both calculate significant intensity in peaks when there is none present, making it clear that they are not appropriate. Conversely the fit obtained using the disordered model in $Pbnm$ contains no significant discrepancies. It should be noted that in the refinement of the $Pbnm$ model the atomic displacement parameter of the disordered Cr/Mn site was fixed at $0.5 \times 10^{-2} \text{ \AA}^3$. The 1:1 mixture of Cr and Mn gives this site an effective neutron scattering length of close to zero.

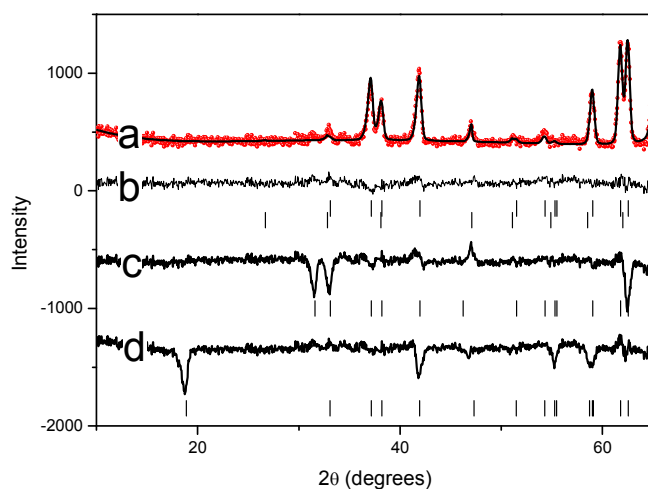


Figure 1. Portion of the neutron diffraction pattern recorded for $\text{YCr}_{0.5}\text{Mn}_{0.5}\text{O}_3$ at room temperature using $\lambda = 2.44 \text{ \AA}$ neutrons. The top trace (a) is the observed data (symbols) and the fit (solid line) to this in the orthorhombic space group $Pbnm$. Below this (trace (b)) is the difference between the observed and calculated profiles in (a) and the tick markers for the (upper) orthorhombic phase and (lower) Y_2O_3 phases. Trace (c) is the difference between the observed data and the best fit in $P2_1/n$, and immediately below are the tick marks showing the positions of the Bragg reflections in $P2_1/n$. Trace (d) is the difference between the observed data and the best fit in $P2_1/b$, and immediately below are the tick marks showing the positions of the Bragg reflections in $P2_1/b$. Although the fits using the monoclinic model both allowed for the presence of trace amounts of Y_2O_3 the tick marks for this phase are not shown below traces (c) and (d) for clarity.

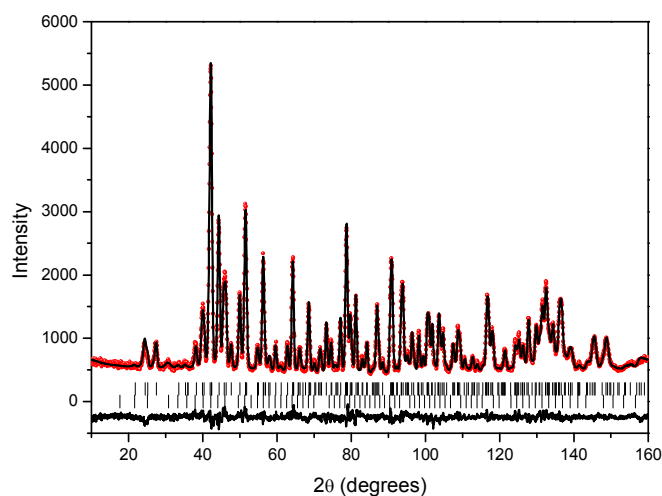


Figure 2. Observed calculated and difference neutron diffraction profiles for $\text{YCr}_{0.5}\text{Mn}_{0.5}\text{O}_3$ at room temperature using $\lambda = 1.62 \text{ \AA}$ neutrons. The structure was refined in the orthorhombic space group $Pbnm$. The lower set of tick marks are from Y_2O_3 .

The refined structural parameters, obtained using a combination of the 1.62 and 2.44 \AA neutron data sets are summarised in Table 1, whilst the fit to the 1.62 \AA pattern is shown in Figure 2. The unit cell parameters in the orthorhombic $Pbnm$ model are related to the unit cell length of the ideal cubic perovskite a_0 as $a \sim \sqrt{2}a_0$, $b \sim \sqrt{2}a_0$, $c \sim 2a_0$ with the expansion in the cell being a consequence of cooperative tilting of the corner sharing $(\text{MnCr})\text{O}_6$ octahedra. The tilting in $Pbnm$ is described as $a^- a^- c^+$ in Glazer's nomenclature. The coordination of the $(\text{MnCr})\text{O}_6$ octahedra is highly distorted with four short and two long $(\text{MnCr})\text{-O}$ bonds $(\text{MnCr})\text{-O}(1)$ 1.9616(4) \AA and $(\text{MnCr})\text{-O}(2)$ 1.9544(10) and 2.0768(11) \AA . This reflects the presence of a Jahn-Teller like distortion associated with the Mn^{3+} cation. That both the Mn and Cr cations are trivalent was verified by Bond Valence calculations that gave a BVS of 3.19 for Mn and 2.90 for Cr. The distortion of the $(\text{MnCr})\text{O}_6$ octahedra is associated with the large pseudo-tetragonal distortion of the unit cell with $\sqrt{2}b/c = 1.06$, This is smaller than the distortion in YMnO_3 , 1.11¹², that only contains Mn^{3+} but is larger than that seen in the Mn^{4+} perovskite CaMnO_3 $b/c = 1.00$ ¹³ or the Cr^{3+} containing oxide YCrO_3 $b/c = 1.04$.¹⁴ A similar large distortion of both the BO_6 octahedra and cell metric was observed in $\text{Sr}_2\text{MnSbO}_6$ where extensive disorder of the Mn^{3+} and Sb^{5+} cations occurs.¹⁵

Table 1. Refined structural parameters for $\text{YCr}_{0.5}\text{Mn}_{0.5}\text{O}_3$ using neutron diffraction data. $a = 5.25074(8)$ $b = 5.62780(10)$ $c = 7.47670(10)$ Å. Volume = $220.937(6)$ Å³. $R_p = 5.40$ $R_{wp} = 4.16$ and $\chi^2 = 2.08$

Name	x	y	z	U _i /U _e *100		
Y	0.01702(20)	0.57255(19)	0.25	0.860(27)		
Cr	0	0	0	0.5 ⁺		
Mn	0	0	0	0.5 ⁺		
O1	-0.10690(24)	-0.03501(25)	0.25	0.79*		
O2	0.19654(18)	0.31212(20)	0.05396(13)	1.02*		
	U ¹¹	U ²²	U ³³	U ¹²	U ¹³	U ²³
O1	0.89(8)	1.16(8)	0.32(7)	0.67(6)	0	0
O2	0.52(4)	1.83(6)	0.71(5)	-0.15(4)	0.08(5)	0.02(5)

+ Fixed at 0.5×10^{-2}

* Anisotropic displacement parameters were employed for the oxygen atoms, whilst that of the disordered Cr/Mn cations was fixed.

Magnetic measurements of $\text{YCr}_{0.5}\text{Mn}_{0.5}\text{O}_3$ reveal a divergence of the zero field cooled and field cooled susceptibilities near 75 K as observed previously. Above 150 K the inverse susceptibilities display Curie-Weiss type behaviour with an effective magnetic moment of $\mu_{\text{eff}} = 4.12\mu_B$ with a negative Weiss constant of $\theta = -57$ K indicative of an antiferromagnetic ground state, although the rapid increase in the field cooled susceptibility is suggestive of ferrimagnetism. The observed magnetic moment and Weiss constant are in excellent agreement with the results described by Liu *et al.* ($4.53 \mu_B$ and -59 K respectively) and the moment is close to the value expected for a 1:1 mixture of Cr^{3+} (d^3) and Mn^{3+} (d^4), $4.39 \mu_B$. The magnetization (M) vs. applied magnetic field (H) measurements at 4 K showed clear hysteresis loops, depicting ferrimagnetic behaviour.

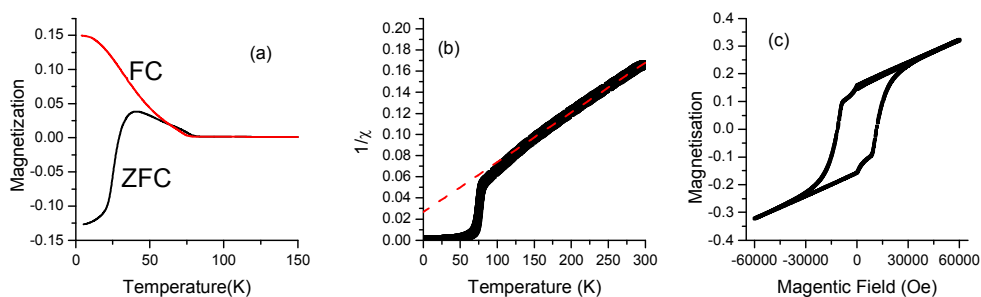


Figure 3 (a) Temperature dependence of the field-cooled (FC) and zero-field-cooled (ZFC) magnetization of $\text{YCr}_{0.5}\text{Mn}_{0.5}\text{O}_3$ was measured at magnetic field of 1 kOe. (b) Temperature dependence of the inverse (FC) molar magnetic susceptibility. The dashed line is a linear fit to the high temperature region. (c) Magnetization as a function of applied magnetic field for $\text{YCr}_{0.5}\text{Mn}_{0.5}\text{O}_3$ at 5 K.

An unusual feature of Figure 3 is the crossover from positive to negative values during the ZFC measurements. As locally $d_{\text{HS}}^4-d_{\text{HS}}^4$, $d_{\text{HS}}^4-d^3$, and d^3-d^3 pairs are expected to couple via superexchange ferro-, ferro-, and antiferromagnetically, respectively, this is believed to be a consequence of magnetic compensation between the Mn^{+3} - Mn^{+3} and Mn^{+3} - Cr^{+3} contact rich domains with the moment aligned antiparallel to each other. We note that the effect of compensation was not observed by Liu³ as it is clearly highly dependent on the sample preparation protocol determining Mn and Cr distribution uniformity over the sample.

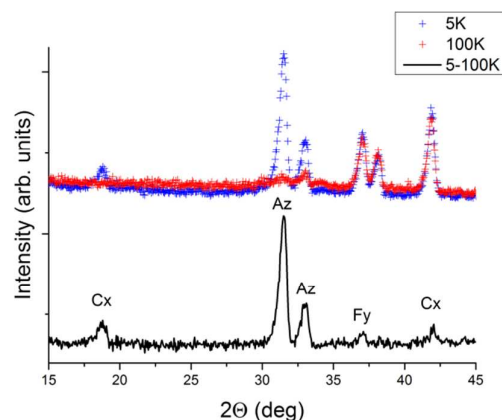


Figure 4. Neutron powder diffraction data collected at 5 K and 100 K and the difference (blue and red symbols and black solid line, respectively). The letters indicate magnetic peaks associated with a particular magnetic ordering mode in the CxFyAz model.

Neutron diffraction measurements at low temperatures showed the presence of magnetic scattering, Figure 4. All the magnetic peaks were indexed by a chemical unit cell i.e. with the propagation vector $k(0,0,0)$. Representational analysis performed with BasiReps for the (4a) Wyckoff site of the space group 62 in the standard $Pnma$ setting revealed AxGyCz , GxAyFz , CxFyAz , and FxCyGz possible ordering models (irreducible representations Γ_1 , Γ_3 , Γ_5 , and Γ_7 , respectively). Data examination showed that the best magnetic model is unambiguously Γ_5 CxFyAz . The structure is best described as G -type, where the AFM component is along c -axis, containing a small ferromagnetic component along the b -axis, see Figure 5.

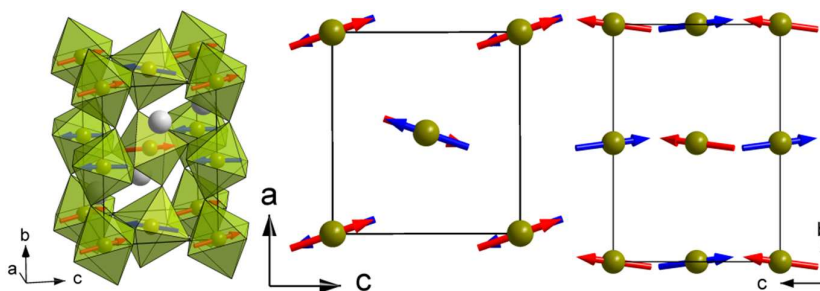


Figure 5. General view of the crystal and magnetic structure of $\text{Y}(\text{Cr}_{0.5}\text{Mn}_{0.5})\text{O}_3$ (left) and projections along b - (middle) and a -axes (right) (in $Pnma$ setting).

In the modelling of the magnetic site it was assumed that the reduction of the moment from the full moment of $S=3/2$ Cr^{3+} and $S=2$ Mn^{3+} is the same for both cations. The final Rietveld plot is shown in Fig. 6. The determined components of magnetic moment along a-, b-, and c-axes are 0.63(3), 0.25(14), 1.83(2) μ_{B} , respectively yielding the total moment of 1.95(3) μ_{B} which is ~ 0.65 of the full moment. The moment reduction is not surprising as locally some Mn^{3+} and Cr^{3+} atoms will have a combination of the nearest magnetic neighbours with interactions of varying strength or even type (AFM/FM).

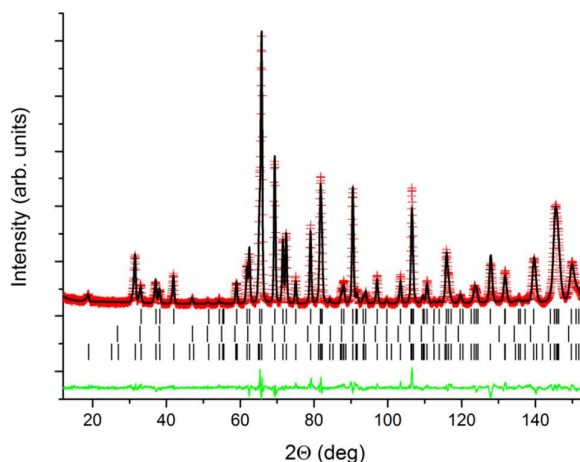


Figure 6. The Rietveld plot for $\text{Y}(\text{Cr}_{0.5}\text{Mn}_{0.5})\text{O}_3$ refined against NPD data collected at 5 K. The red crosses and black and green solid lines indicate the observed and calculated patterns and their difference, respectively. The tick marks from top to bottom indicate the position of the diffraction peaks of the nuclear structures of $\text{Y}(\text{Cr}_{0.5}\text{Mn}_{0.5})\text{O}_3$, Y_2O_3 (0.53(5)wt.%), and magnetic structure of $\text{Y}(\text{Cr}_{0.5}\text{Mn}_{0.5})\text{O}_3$. $R_p = 4.53\%$, $R_{wp} = 5.93\%$, $R_{mag} = 6.14\%$, $\chi^2 = 3.10$.

Finally, the model indeed allows ferromagnetic component (along b-axis) and then we have two options: either Cr and Mn are coupled ferro- or ferri- to each other. The data does not allow these options to be distinguished. That such coupling can exist in the disordered model was overlooked by Hiu *et al.*^{4,5}

Conclusions

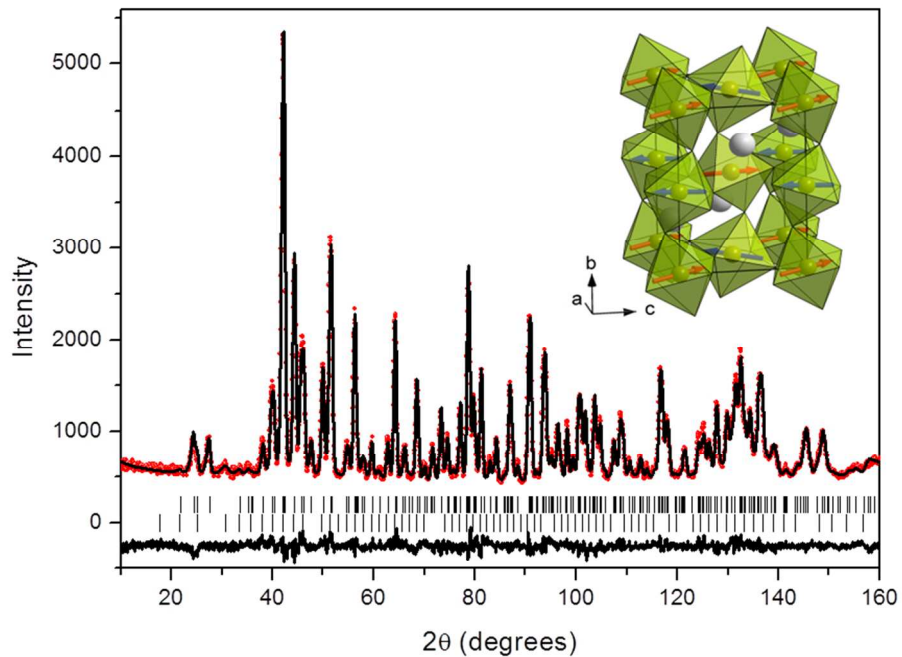
Neutron diffraction measurements show that the structure of the perovskite $\text{YCr}_{0.5}\text{Mn}_{0.5}\text{O}_6$ is adequately described in the orthorhombic space group $Pbnm$, in which the Cr^{3+} and Mn^{3+} cations randomly occupy the octahedral sites. Whilst it is possible altering the conditions used to prepare the sample can alter the degree of disorder, the neutron data demonstrate that the previous suggestion of ordering of the Cr^{3+} and Mn^{3+} cations is incorrect. Magnetic susceptibility measurements confirm the presence of magnetic ordering. Low temperature neutron diffraction data reveal that the strongest magnetic exchange is indicative of a G-type antiferromagnetic type arrangement. These data reveal the presence of a ferromagnetic component along the b-axis, indicating that the Cr and Mn couple ferro (or possibly ferri) magnetically to each other.

Acknowledgments

We acknowledge the Australian Research Council and the Australian Institute of Nuclear Science and Engineering for support of this work.

References

1. J. M. D. Coey, M. Viret and S. von Molnar, *Advances in Physics*, 1999, **48**, 167-293.
2. Z. Popovic and S. Satpathy, *Phys. Rev. Lett.*, 2002, **88**, 197201.
3. F. Y. Liu, J. J. Li, Q. L. Li, Y. Wang, X. D. Zhao, Y. J. Hua, C. T. Wang and X. Y. Liu, *Dalton Trans.*, 2014, **43**, 1691-1698.
4. L. Yang, Q. Y. Duanmu, L. Hao, Z. F. Zhang, X. P. Wang, Y. Y. Wei and H. Zhu, *Journal of Alloys and Compounds*, 2013, **570**, 41-45.
5. L. Hao, L. Yang, M. H. Lee, T. H. Lin, Z. F. Zhang, X. N. Xie and H. Zhu, *Journal of Alloys and Compounds*, 2014, **601**, 14-18.
6. M. T. Anderson, K. B. Greenwood, G. A. Taylor and K. R. Poeppelmeier, *Prog. Solid State Chem.*, 1993, **22**, 197-233.
7. Q. D. Zhou, B. J. Kennedy, C. J. Howard, M. M. Elcombe and A. J. Studer, *Chem. Mat.*, 2005, **17**, 5357-5365.
8. B. J. Kennedy, C. J. Howard, K. S. Knight, Z. M. Zhang and Q. D. Zhou, *Acta Crystallogr. Sect. B-Struct. Commun.*, 2006, **62**, 537-546.
9. S. Miyasaka, Y. Okimoto, M. Iwama and Y. Tokura, *Physical Review B*, 2003, **68**, 100406.
10. K. L. Kobayashi, T. Kimura, H. Sawada, K. Terakura and Y. Tokura, *Nature*, 1998, **395**, 677-680.
11. K. D. Liss, B. Hunter, M. Hagen, T. Noakes and S. Kennedy, *Physica B*, 2006, **385-86**, 1010-1012.
12. J. A. Alonso, M. J. Martinez-Lope, M. T. Casais and M. T. Fernandez-Diaz, *Inorg. Chem.*, 2000, **39**, 917-923.
13. Q. D. Zhou and B. J. Kennedy, *J. Phys. Chem. Solids*, 2006, **67**, 1595-1598.
14. K. Sardar, M. R. Lees, R. J. Kashtiban, J. Sloan and R. I. Walton, *Chem. Mat.*, 2011, **23**, 48-56.
15. M. Cheah, P. J. Saines and B. J. Kennedy, *J. Solid State Chem.*, 2006, **179**, 1775-1781.



Neutron Powder diffraction demonstrates cation disorder in $\text{YCr}_{0.5}\text{Mn}_{0.5}\text{O}_6$ in a G-type antiferromagnetic arrangement.
254x190mm (96 x 96 DPI)